

An embedded–hybridized discontinuous Galerkin finite element method for the Stokes equations

Sander Rhebergen^{a,1}, Garth N. Wells^{b,2}

^a*Department of Applied Mathematics, University of Waterloo, Canada*

^b*Department of Engineering, University of Cambridge, United Kingdom*

Abstract

We present and analyze a new embedded–hybridized discontinuous Galerkin finite element method for the Stokes problem. The method has the attractive properties of full hybridized methods, namely an $H(\text{div})$ -conforming velocity field, pointwise satisfaction of the continuity equation and *a priori* error estimates for the velocity that are independent of the pressure. The embedded–hybridized formulation has advantages over a full hybridized formulation in that it has fewer global degrees-of-freedom for a given mesh and the algebraic structure of the resulting linear system is better suited to fast iterative solvers. The analysis results are supported by a range of numerical examples that demonstrate rates of convergence, and which show computational efficiency gains over a full hybridized formulation.

Keywords: Stokes equations, preconditioning, embedded, hybridized, discontinuous Galerkin finite element methods.

2010 MSC: 65F08, 65M15, 65N12, 65N30, 76D07.

1. Introduction

Hybridized discontinuous Galerkin (HDG) methods were introduced with the purpose of reducing the computational cost of discontinuous Galerkin methods while retaining the attractive features. HDG methods for the Stokes equations were introduced in [1] for the vorticity-velocity-pressure formulation of the Stokes problem, and a modified version of this method for the velocity-pressure-gradient formulation of the Stokes equations was introduced and analyzed in [2, 3, 4]. An HDG method for the velocity-pressure formulation of the Stokes equations was analyzed in [5]. To lower the computational cost of HDG methods, embedded discontinuous Galerkin (EDG) [6] methods for incompressible flows have been developed which retain many of the attractive features of discontinuous Galerkin methods but with the same number of global degrees of freedom as a continuous Galerkin method on a given mesh [7, 8]. The main difference between EDG and HDG methods is the choice of function spaces for the facet Lagrange multipliers. In the case of an HDG method, the Lagrange multipliers are discontinuous between facets. To reduce the number of degrees-of-freedom for a given mesh one may use continuous Lagrange multipliers, leading to an EDG method.

Email addresses: srheberg@uwaterloo.ca (Sander Rhebergen), gnw20@cam.ac.uk (Garth N. Wells)

¹<https://orcid.org/0000-0001-6036-0356>

²<https://orcid.org/0000-0001-5291-7951>

The HDG method reduces the computational cost of discontinuous Galerkin methods by introducing facet variables and eliminating local (cell-wise) degrees-of-freedom, following ideas originally introduced for mixed finite element methods, e.g. [9]. This static condensation can significantly reduce the size of the global problem for higher-order discretizations. It is possible to reduce the problem size of $H(\text{div})$ -conforming HDG methods further by exploiting that the normal component of the velocity is continuous across facets. These methods only require to enforce continuity in the tangential direction of the facet velocity [10, 11]. By the *projected jumps* method, in which the polynomial degree of the tangential facet velocity is reduced by one compared to the cell velocity approximation, [10, 11] were able to lower the number of globally coupled degrees-of-freedom even more. An alternative to increase the performance of HDG methods is by a cell-wise post-processing. For diffusion dominated, incompressible flows, post-processing techniques have been introduced that result in super-convergent, $H(\text{div})$ -conforming, and point-wise divergence-free velocity fields, see for example [12, 2].

A property that we are particularly interested in is *pressure robustness*, which is when the *a priori* error estimate for the velocity does not depend on the pressure error (scaled by the inverse of the viscosity). A way to achieve pressure robustness is to devise a finite element method with an $H(\text{div})$ -conforming and divergence-free velocity approximation. In a series of papers, Cockburn et al. [13, 14, 15, 16] introduced an $H(\text{div})$ -conforming discontinuous Galerkin method for incompressible flows (see also [17]). $H(\text{div})$ -conforming and divergence-free HDG methods were introduced and analysed for incompressible flows by, for example [18, 10, 11, 19, 5, 20]. For other $H(\text{div})$ -conforming finite element methods we refer to, for example, [21, 22, 23, 24, 25] and the review paper by John et al. [26]. When a method is not $H(\text{div})$ -conforming, reconstruction operators [22, 24] or post-processing [15, 27] of the approximate velocity field can be used to achieve pressure robustness.

Embedded discontinuous Galerkin (EDG) methods use continuous Lagrange multipliers on facets, thereby reducing the number of globally coupled degrees-of-freedom compared to HDG methods. However, some attractive properties are lost. It was shown, for example, that there is no post-processing of EDG methods that result in super-convergent solutions [28]. Moreover, the approximate velocity field is not $H(\text{div})$ -conforming and as consequence the EDG method is not pressure robust. In the context of the incompressible Navier–Stokes equations, mass and momentum conservation cannot be satisfied simultaneously [8].

The number of globally coupled degrees-of-freedom alone is not necessarily a good proxy for efficiency; efficiency will also depend on the performance of linear solvers. We formulate and analyze a new EDG–HDG method that retains the pressure-robustness property of HDG methods, and has the efficiency characteristics of EDG methods. The method yields a velocity field that is pointwise divergence-free and automatically $H(\text{div})$ -conforming. This is achieved through hybridization via a facet pressure field that is discontinuous between facets, as is typical for HDG methods. For the facet velocity field, we use a continuous basis. This is desirable for substantially reducing the number of global velocity degrees-of-freedom on a given mesh, and continuous methods are generally observed to lead to better performance of preconditioned iterative solvers. We present analysis for the EDG, EDG–HDG and HDG formulations of the Stokes problem in a unified setting. In particular, the analysis highlights key differences between the methods in the context of pressure robustness.

We test performance numerically using the preconditioner developed and analyzed in [29]. As anticipated, the preconditioner is more effective in terms of lower iteration counts for the more

regular EDG–HDG method compared to the HDG method. The fewer linear solver iterations combined with the fewer global degrees-of-freedom for the EDG–HDG method compared to the HDG method lead to the observation via numerical experiments that the EDG–HDG method is considerably more efficient in terms of the time required to reach a given discretization error. It should be mentioned that our numerical experiments only compare the ‘standard’ EDG, HDG and EDG–HDG methods without taking advantage of any modifications that can be made to reduce the problem size even further, such as the projected jumps method. As such, these numerical experiments serve to indicate the speed-up that is possible when exploiting the ‘continuous’ structure built into the EDG and EDG–HDG methods compared to the HDG method.

The remainder of this article is organized as follows. In section 2 we introduce the HDG, EDG and EDG–HDG methods for the Stokes problem, and we prove inf-sup stability for all three methods. Error estimates are provided in section 3, and in particular pressure robustness of the HDG and EDG–HDG methods is considered. The error estimates are supported by numerical examples in section 4.1. Preconditioning is discussed in section 4.4, with performance of the different methods with preconditioned solvers examined by numerical examples. Conclusions are drawn in section 5.

2. The hybridized, embedded and embedded-hybridized discontinuous Galerkin method

In this section we consider the embedded, hybridized, and embedded–hybridized discontinuous Galerkin methods for the Stokes problem:

$$-\nu \nabla^2 u + \nabla p = f \quad \text{in } \Omega, \quad (1a)$$

$$\nabla \cdot u = 0 \quad \text{in } \Omega, \quad (1b)$$

$$u = 0 \quad \text{on } \partial\Omega, \quad (1c)$$

$$\int_{\Omega} p \, dx = 0, \quad (1d)$$

where $\Omega \subset \mathbb{R}^d$ is a polygonal ($d = 2$) or polyhedral ($d = 3$) domain, $u : \Omega \rightarrow \mathbb{R}^d$ is the velocity, $p : \Omega \rightarrow \mathbb{R}$ is the pressure, $f : \Omega \rightarrow \mathbb{R}^d$ is the prescribed body force, and $\nu \in \mathbb{R}^+$ is a given constant kinematic viscosity.

2.1. Notation

Let $\mathcal{T} := \{K\}$ be a triangulation of Ω . This triangulation consists of non-overlapping simplicial cells K . The length measure of a cell K is denoted by h_K . The outward unit normal vector, on the boundary of a cell, ∂K , is denoted by n . An interior facet F is shared by two adjacent cells K^+ and K^- while a boundary facet is a facet of ∂K that lies on $\partial\Omega$. The set and union of all facets are denoted by, respectively, $\mathcal{F} = \{F\}$ and Γ_0 .

We consider the following discontinuous finite element function spaces on Ω :

$$\begin{aligned} V_h &:= \left\{ v_h \in [L^2(\Omega)]^d : v_h \in [P_k(K)]^d, \forall K \in \mathcal{T} \right\}, \\ Q_h &:= \left\{ q_h \in L^2(\Omega) : q_h \in P_{k-1}(K), \forall K \in \mathcal{T} \right\}, \end{aligned} \quad (2)$$

where $P_k(K)$ denotes the set of polynomials of degree k on a cell K . On Γ_0 we consider the finite element spaces

$$\begin{aligned}\bar{V}_h &:= \left\{ \bar{v}_h \in [L^2(\Gamma_0)]^d : \bar{v}_h \in [P_k(F)]^d \ \forall F \in \mathcal{F}, \bar{v}_h = 0 \text{ on } \partial\Omega \right\}, \\ \bar{Q}_h &:= \left\{ \bar{q}_h \in L^2(\Gamma_0) : \bar{q}_h \in P_k(F) \ \forall F \in \mathcal{F} \right\},\end{aligned}\tag{3}$$

where $P_k(F)$ denotes the set of polynomials of degree k on a facet F . We also introduce the extended function spaces

$$V(h) := V_h + [H_0^1(\Omega)]^d \cap [H^2(\Omega)]^d,\tag{4}$$

$$Q(h) := Q_h + L_0^2(\Omega) \cap H^1(\Omega),\tag{5}$$

and

$$\bar{V}(h) := \bar{V}_h + [H_0^{3/2}(\Gamma_0)]^d,\tag{6}$$

$$\bar{Q}(h) := \bar{Q}_h + H_0^{1/2}(\Gamma_0).\tag{7}$$

We define two norms on $V(h) \times \bar{V}(h)$, namely,

$$\|\mathbf{v}\|_v^2 := \sum_{K \in \mathcal{T}} \|\nabla v\|_K^2 + \sum_{K \in \mathcal{T}} \frac{\alpha_v}{h_K} \|\bar{v} - v\|_{\partial K}^2,\tag{8}$$

and

$$\|\mathbf{v}\|_{v'}^2 := \|\mathbf{v}\|_v^2 + \sum_{K \in \mathcal{T}} \frac{h_K}{\alpha_v} \left\| \frac{\partial v}{\partial n} \right\|_{\partial K}^2,\tag{9}$$

where $\alpha_v > 0$ is a penalty parameter that will be defined later. From the discrete trace inequality [30, Remark 1.47],

$$h_K^{1/2} \|v_h\|_{\partial K} \leq C_t \|v_h\|_K \quad \forall v_h \in P_k(K),\tag{10}$$

where C_t depends on k , spatial dimension and cell shape, it follows that the norms $\|\cdot\|_v$ and $\|\cdot\|_{v'}$ are equivalent on the finite element space $V_h \times \bar{V}_h$:

$$\|\mathbf{v}_h\|_v \leq \|\mathbf{v}_h\|_{v'} \leq c(1 + \alpha_v^{-1}) \|\mathbf{v}_h\|_v \quad \forall \mathbf{v}_h \in V_h \times \bar{V}_h,\tag{11}$$

where $c > 0$ a constant independent of h , see [31, Eq. (5.5)].

On $\bar{Q}(h)$ and $Q(h) \times \bar{Q}(h)$ we introduce, respectively,

$$\|\bar{q}\|_p^2 := \sum_{K \in \mathcal{T}} h_K \|\bar{q}\|_{\partial K}^2, \quad \|\mathbf{q}\|_p^2 := \|q\|_\Omega^2 + \|\bar{q}\|_p^2.\tag{12}$$

2.2. Weak formulation

Consider the bilinear form

$$B_h((\mathbf{u}_h, \mathbf{p}_h), (\mathbf{v}_h, \mathbf{q}_h)) := a_h(\mathbf{u}_h, \mathbf{v}_h) + b_h(\mathbf{p}_h, v_h) - b_h(\mathbf{q}_h, u_h),\tag{13}$$

where

$$a_h(\mathbf{u}, \mathbf{v}) := \sum_{K \in \mathcal{T}} \int_K \nu \nabla \mathbf{u} : \nabla \mathbf{v} \, dx + \sum_{K \in \mathcal{T}} \int_{\partial K} \frac{\nu \alpha_v}{h_K} (u - \bar{u}) \cdot (v - \bar{v}) \, ds \quad (14a)$$

$$- \sum_{K \in \mathcal{T}} \int_{\partial K} \nu \left[(u - \bar{u}) \cdot \frac{\partial v}{\partial n} + \frac{\partial u}{\partial n} \cdot (v - \bar{v}) \right] \, ds,$$

$$b_h(\mathbf{p}, v) := - \sum_{K \in \mathcal{T}} \int_K p \nabla \cdot v \, dx + \sum_{K \in \mathcal{T}} \int_{\partial K} v \cdot n \bar{p} \, ds. \quad (14b)$$

The methods involve: find $(\mathbf{u}_h, \mathbf{p}_h) \in X_h$ such that

$$B_h((\mathbf{u}_h, \mathbf{p}_h), (\mathbf{v}_h, \mathbf{q}_h)) = \int_{\Omega} f \cdot v_h \, dx \quad \forall (\mathbf{v}_h, \mathbf{q}_h) \in X_h, \quad (15)$$

where $X_h = X_h^v \times X_h^q$, and the different formulations use the following spaces:

$$X_h := \begin{cases} (V_h \times \bar{V}_h) \times (Q_h \times \bar{Q}_h) & \text{HDG method,} \\ (V_h \times (\bar{V}_h \cap C^0(\Gamma_0))) \times (Q_h \times \bar{Q}_h) & \text{EDG–HDG method,} \\ (V_h \times (\bar{V}_h \cap C^0(\Gamma_0))) \times (Q_h \times (\bar{Q}_h \cap C^0(\Gamma_0))) & \text{EDG method.} \end{cases} \quad (16)$$

The HDG method uses facet function spaces that are discontinuous. In the EDG–HDG method the facet velocity field is continuous and the facet pressure field is discontinuous, and in the EDG method both velocity and pressure facet functions are continuous.

All three formulations yield computed velocity fields that are pointwise solenoidal on cells. This is an immediate consequence of $\nabla \cdot v_h \in Q_h$ for all $v_h \in V_h$. For the HDG and EDG–HDG formulations the facet pressure is discontinuous (lying in \bar{Q}_h), in which case it is straightforward to show that $u_h \in H(\text{div}, \Omega)$, i.e. the normal component of the computed velocity u_h is continuous across cell facets [5]. We will therefore refer to the HDG and EDG–HDG methods as being *H(div)-conforming*. In the case of the EDG method, the normal component of the velocity is only weakly continuous across cell facets.

The HDG variant of the formulation was analyzed in [5], but pressure robustness, in which the *a priori* error estimate for the velocity does not depend on the pressure error, was not proven. We generalize and extend analysis results to include the EDG and EDG–HDG formulations, and to prove pressure robustness of the HDG and EDG–HDG formulations. In the following analysis we present, where possible, results that hold without reference to a specific method. Where this is not possible we comment explicitly on the conditions for a result to hold for a specific method.

2.3. Consistency

We consider the following space for the exact solution to the Stokes problem:

$$X := \left([H_0^1(\Omega)]^d \cap [H^2(\Omega)]^d \right) \times \left(L_0^2(\Omega) \cap H^1(\Omega) \right). \quad (17)$$

Lemma 1. *Let $(u, p) \in X$ solve the Stokes problem eq. (1) and let $\mathbf{u} = (u, u)$ and $\mathbf{p} = (p, p)$. Then*

$$B_h((\mathbf{u}, \mathbf{p}), (\mathbf{v}_h, \mathbf{q}_h)) = \int_{\Omega} f \cdot v_h \, dx \quad \forall (\mathbf{v}_h, \mathbf{q}_h) \in X_h. \quad (18)$$

PROOF. See [5, Lemma 3.1]. □

The result in [5, Lemma 3.1] holds trivially for the EDG–HDG and EDG methods as they involve subspaces of the HDG method.

2.4. Stability and boundedness

Stability and boundedness of the vector-Laplacian term, a_h , for the EDG and EDG–HDG method is a direct consequence of the stability and boundedness results of the HDG method proven in [5]. We state these results here for completeness.

Lemma 2 (Stability of a_h). *There exists a $\beta_v > 0$, independent of h , and a constant $\alpha_0 > 0$ such that for $\alpha_v > \alpha_0$ and for all $\mathbf{v}_h \in V_h \times \bar{V}_h$*

$$a_h(\mathbf{v}_h, \mathbf{v}_h) \geq \nu \beta_v \|\mathbf{v}_h\|_v^2. \quad (19)$$

PROOF. See [5, Lemma 4.2]. □

Lemma 3 (Boundedness of a_h). *There exists a $c > 0$, independent of h , such that for all $\mathbf{u} \in V(h) \times \bar{V}(h)$ and for all $\mathbf{v}_h \in V_h \times \bar{V}_h$*

$$|a_h(\mathbf{u}, \mathbf{v}_h)| \leq C_a \nu \|\mathbf{u}\|_{v'} \|\mathbf{v}_h\|_v, \quad (20)$$

with $C_a = c(1 + \alpha_v^{-1/2})$.

PROOF. See [5, Lemma 4.3]. □

Lemmas 2 and 3 hold trivially for the EDG–HDG and EDG formulations as velocity fields in both cases are subspaces of $V_h \times \bar{V}_h$.

The velocity-pressure coupling in eq. (15) is provided by:

$$b_h(\mathbf{p}_h, v_h) := b_1(p_h, v_h) + b_2(\bar{p}_h, v_h), \quad (21)$$

where

$$b_1(p_h, v_h) := - \sum_{K \in \mathcal{T}} \int_K p_h \nabla \cdot v_h \, dx \quad \text{and} \quad b_2(\bar{p}_h, v_h) := \sum_{K \in \mathcal{T}} \int_{\partial K} v_h \cdot n \bar{p}_h \, ds. \quad (22)$$

We consider the inf-sup condition for b_1 and b_2 separately first, after which we prove inf-sup stability for b_h .

It is useful to introduce the Brezzi–Douglas–Marini (BDM) finite element space, V_h^{BDM} (see [9]):

$$\begin{aligned} V_h^{\text{BDM}}(K) &:= \left\{ v_h \in [P_k(K)]^d : v_h \cdot n \in L^2(\partial K), v_h \cdot n|_F \in P_k(F) \right\}, \\ V_h^{\text{BDM}} &:= \left\{ v_h \in H(\text{div}; \Omega) : v_h|_K \in V_h^{\text{BDM}}(K) \, \forall K \in \mathcal{T} \right\}, \end{aligned} \quad (23)$$

and the following interpolation operator [32, Lemma 7].

Lemma 4. *If the mesh consists of triangles in two dimensions or tetrahedra in three dimensions there is an interpolation operator $\Pi_{\text{BDM}} : [H^1(\Omega)]^d \rightarrow V_h$ with the following properties for all $u \in [H^{k+1}(K)]^d$ where $k \geq 1$:*

(i) $[[n \cdot \Pi_{\text{BDM}}u]] = 0$, where $[[a]] = a^+ + a^-$ and $[[a]] = a$ on, respectively, interior and boundary faces is the usual jump operator.

(ii) $\|u - \Pi_{\text{BDM}}u\|_{m,K} \leq ch_K^{l-m} \|u\|_{l,K}$ with $m = 0, 1, 2$ and $m \leq l \leq k + 1$.

(iii) $\|\nabla \cdot (u - \Pi_{\text{BDM}}u)\|_{m,K} \leq ch_K^{l-m} \|\nabla \cdot u\|_{l,K}$ with $m = 0, 1$ and $m \leq l \leq k$.

(iv) $\int_K q(\nabla \cdot u - \nabla \cdot \Pi_{\text{BDM}}u) dx = 0$ for all $q \in P_{k-1}(K)$.

(v) $\int_F \bar{q}(n \cdot u - n \cdot \Pi_{\text{BDM}}u) ds = 0$ for all $\bar{q} \in P_k(F)$, where F is a face on ∂K .

We will also use an interpolation operator $\mathcal{I}_h : H^1(\Omega) \rightarrow V_h \cap C^0(\bar{\Omega})$ with the following property:

$$\sum_K h_K^{-2} \|v - \mathcal{I}_h v\|_{0,K}^2 \leq c|v|_{1,\Omega}^2, \quad (24)$$

for example, the Scott–Zhang interpolant (see [33, Theroem 4.8.12]).

Lemma 5 (Stability of b_1). *There exists a constant $\beta_1 > 0$, independent of h , such that for all $q_h \in Q_h$*

$$\beta_1 \|q_h\|_{\Omega} \leq \sup_{\mathbf{v}_h \in V_h^{\text{BDM}} \times (\bar{V}_h \cap C^0(\Gamma_0))} \frac{b_1(q_h, v_h)}{\|\mathbf{v}_h\|_v}. \quad (25)$$

PROOF. We first consider a bound for $\|\cdot\|_v$. From item ii of lemma 4 and the triangle inequality,

$$\|\nabla(\Pi_{\text{BDM}}v)\|_K \leq \|\nabla v - \nabla(\Pi_{\text{BDM}}v)\|_K + \|\nabla v\|_K \leq c\|v\|_{1,K}, \quad (26)$$

and

$$\sum_K h^{-1} \|\Pi_{\text{BDM}}v - \mathcal{I}_v v\|_{0,\partial K}^2 \leq \sum_K ch^{-2} \|\Pi_{\text{BDM}}v - \mathcal{I}_v v\|_{0,K}^2 \leq c\|v\|_{1,K}^2 \quad (27)$$

for all $v \in [H^1(\Omega)]^d$, where in eq. (27) the first inequality is due to the trace inequality eq. (10), and the second is due to item ii of lemma 4 and the interpolation estimate in eq. (24). Combining eqs. (26) and (27),

$$\|(\Pi_{\text{BDM}}v, \mathcal{I}_h v)\|_v^2 \leq c(1 + \alpha_v) \|v\|_{1,\Omega}^2 \quad \forall v \in [H^1(\Omega)]^d. \quad (28)$$

For all $q \in L_0^2(\Omega)$ there exists a $v_q \in [H_0^1(\Omega)]^d$ such that

$$q = \nabla \cdot v_q \quad \text{and} \quad \beta_c \|v_q\|_{1,\Omega} \leq \|q\|_{\Omega}, \quad (29)$$

where $\beta_c > 0$ is a constant depending only on Ω (see, e.g. [30, Theorem 6.5]). For $q_h \in Q_h$, we denote $v_{q_h} \in [H_0^1(\Omega)]^d$ such that $\nabla \cdot v_{q_h} = q_h$. It then follows that

$$\|q_h\|_{\Omega}^2 = \int_{\Omega} q_h \nabla \cdot v_{q_h} dx = \int_{\Omega} q_h \nabla \cdot \Pi_{\text{BDM}}v_{q_h} dx = -b_1(q_h, \Pi_{\text{BDM}}v_{q_h}) \quad (30)$$

by item iv of lemma 4 and by the definition of b_1 in eq. (22), and from eq. (28),

$$\|(\Pi_{\text{BDM}}v_{q_h}, \mathcal{I}_h v_{q_h})\|_v \leq c\sqrt{1 + \alpha_v} \|v_{q_h}\|_{1,\Omega} \leq c\sqrt{1 + \alpha_v} \beta_c^{-1} \|q_h\|_{\Omega}. \quad (31)$$

Satisfaction of eq. (25) follows from

$$\sup_{\mathbf{v}_h \in V_h^{\text{BDM}} \times (\bar{V}_h \cap C^0(\Gamma_0))} \frac{-b_1(q_h, v_h)}{\|\mathbf{v}_h\|_v} \geq \frac{-b_1(q_h, \Pi_{\text{BDM}} v_{q_h})}{\|(\Pi_{\text{BDM}} v_{q_h}, \mathcal{I}_h^k v_{q_h})\|_v} \geq \frac{\beta_c}{c\sqrt{1 + \alpha_v}} \|q_h\|_\Omega, \quad (32)$$

where $\nabla \cdot v_{q_h} = q_h$, and where eqs. (30) and (31) are used for the second inequality. \square

The preceding proof is simpler and more general than [5, Lemma 4.4], which was for the case of discontinuous facet functions, i.e., $\mathbf{v}_h \in V_h^{\text{BDM}} \times \bar{V}_h$.

Lemma 6 (Stability of b_2). *There exists a constant $\beta_2 > 0$, independent of h , such that for all $\bar{q}_h \in \bar{Q}_h$*

$$\beta_2 \|\bar{q}_h\|_p \leq \sup_{\mathbf{v}_h \in V_h \times (\bar{V}_h \cap C^0(\Gamma_0))} \frac{b_2(\bar{q}_h, v_h)}{\|\mathbf{v}_h\|_v}. \quad (33)$$

PROOF. Note that

$$\beta_2 \|\bar{q}_h\|_p \leq \sup_{v_h \in V_h} \frac{b_2(\bar{q}_h, v_h)}{\|(v_h, 0)\|_v} \leq \sup_{\mathbf{v}_h \in V_h \times (\bar{V}_h \cap C^0(\Gamma_0))} \frac{b_2(\bar{q}_h, v_h)}{\|\mathbf{v}_h\|_v}, \quad (34)$$

where the first inequality was proven in [29, Lemma 3]. \square

Lemma 7 (Boundedness of b_1 and b_2). *There exists a $C_b > 0$, independent of h , such that for all $\mathbf{v}_h \in V_h \times \bar{V}_h$ and for all $\mathbf{q}_h \in Q_h \times \bar{Q}_h$*

$$|b_1(q_h, v_h)| \leq \|\mathbf{v}_h\|_v \|\mathbf{q}_h\|_p \quad \text{and} \quad |b_2(\bar{q}_h, v_h)| \leq C_b \|\mathbf{v}_h\|_v \|\mathbf{q}_h\|_p. \quad (35)$$

PROOF. The proof is identical to that of [5, Lemma 4.8]. \square

Lemma 7 holds trivially for the EDG–HDG and EDG formulations as the velocity and pressure fields in both cases are subspaces of $V_h \times \bar{V}_h$ and $Q_h \times \bar{Q}_h$, respectively.

The following is a reduced version of [34, Theorem 3.1] and will be used to prove stability of the combined pressure coupling term.

Theorem 1. *Let U , P_1 , and P_2 be reflexive Banach spaces, and let $b_1 : P_1 \times U \rightarrow \mathbb{R}$, and $b_2 : P_2 \times U \rightarrow \mathbb{R}$ be bilinear and bounded. Let*

$$Z_{b_2} := \{v \in U : b_2(p_i, v) = 0 \quad \forall p_2 \in P_2\} \subset U, \quad (36)$$

then the following are equivalent:

1. *There exists $c > 0$ such that*

$$\sup_{v \in U} \frac{b_1(p_1, v) + b_2(p_2, v)}{\|v\|_U} \geq c \left(\|p_1\|_{P_1} + \|p_2\|_{P_2} \right) \quad (p_1, p_2) \in P_1 \times P_2.$$

2. *There exists $c > 0$ such that*

$$\sup_{v \in Z_{b_2}} \frac{b_1(p_1, v)}{\|v\|_U} \geq c \|p_1\|_{P_1}, \quad p_1 \in P_1 \quad \text{and} \quad \sup_{v \in U} \frac{b_2(p_2, v)}{\|v\|_U} \geq c \|p_2\|_{P_2}, \quad p_2 \in P_2.$$

Lemma 8 (Stability of b_h). *There exists constant $\beta_p > 0$, independent of h , such that for all $\mathbf{q}_h \in Q_h \times \bar{Q}_h$*

$$\beta_p \|\mathbf{q}_h\|_p \leq \sup_{\mathbf{v}_h \in V_h \times (\bar{V}_h \cap C^0(\Gamma_0))} \frac{b_h(\mathbf{q}_h, \mathbf{v}_h)}{\|\mathbf{v}_h\|_v}. \quad (37)$$

PROOF. Let $b_1(\cdot, \cdot)$ and $b_2(\cdot, \cdot)$ be defined as in eq. (22), and let $U := V_h \times (\bar{V}_h \cap C^0(\Gamma_0))$, $P_1 := Q_h$, $P_2 := \bar{Q}_h$ and $Z_{b_2} := V_h^{\text{BDM}} \times (\bar{V}_h \cap C^0(\Gamma_0))$. This definition of Z_{b_2} satisfies eq. (36) by virtue of continuity of the normal component of functions in V_h^{BDM} across facets. The conditions in item 2 of theorem 1 are satisfied by lemmas 5 and 6. The result follows by equivalence of items 1 and 2 in theorem 1. \square

Lemma 8 is posed for the EDG–HDG case, but holds trivially for the HDG case with a larger facet velocity space, $\mathbf{v}_h \in V_h \times \bar{V}_h \supset V_h \times (\bar{V}_h \cap C^0(\Gamma_0))$, and for the EDG method with a smaller facet pressure space, $\mathbf{q}_h \in Q_h \times (\bar{Q}_h \cap C^0(\Gamma_0)) \subset Q_h \times \bar{Q}_h$.

An immediate consequence of the stability of a_h (lemma 2) and the stability of b_h (lemma 8) is that the discrete problem in eq. (15) is well-posed, see, e.g. [35, Theorem 2.4].

3. Error estimates and pressure robustness

Convergence is an immediate consequence of the stability and boundedness results. Let $(u, p) \in [H^{k+1}(\Omega)]^d \times H^k(\Omega)$ $k \geq 1$ solve the Stokes problem eq. (1), and let $\mathbf{u} = (u, u)$ and $\mathbf{p} = (p, p)$. If $(\mathbf{u}_h, \mathbf{p}_h) \in X_h$ solves the finite element problem in eq. (15), then there exists a constant $c > 0$, independent of h , such that

$$\nu^{1/2} \|\mathbf{u} - \mathbf{u}_h\|_v + \nu^{-1/2} \|\mathbf{p} - \mathbf{p}_h\|_p \leq c \left(h^k \nu^{1/2} \|u\|_{k+1, \Omega} + h^k \nu^{-1/2} \|p\|_{k, \Omega} \right). \quad (38)$$

A proof of this estimate is a simple extension of the proof given for the HDG discretization of the Stokes problem in [5, Section 5].

The error estimate in eq. (38) involves norms of the velocity and pressure fields, and concerningly the norm of the exact pressure scaled by $\nu^{-1/2}$. For the HDG and the EDG–HDG cases, but not for the EDG case, an improved estimate for the velocity field can be found that does not depend on the pressure. The improved estimate relies on the velocity field being pointwise divergence-free and $H(\text{div})$ -conforming (the latter condition not being met by the EDG method).

Theorem 2 (Pressure robust error estimate). *Let $u \in [H^{k+1}(\Omega)]^d$ be the velocity solution of the Stokes problem eq. (1) with $k \geq 1$, let $\mathbf{u} = (u, u)$, and let $\mathbf{u}_h \in X_h^v$ be the velocity solution of the finite element problem eq. (15) for the HDG or EDG–HDG formulations. There exists a constant $C > 0$, independent of h , such that*

$$\|\mathbf{u} - \mathbf{u}_h\|_v \leq Ch^k \|u\|_{k+1, \Omega}. \quad (39)$$

PROOF. Consider $\mathbf{w}_h := \mathbf{u}_h - \mathbf{v}_h \in X_h^v$, subject to $b_h(\mathbf{q}_h, \mathbf{w}_h) = 0 \forall \mathbf{q}_h \in X_h^q$. From lemmas 2 and 3 it holds that for all \mathbf{v}_h :

$$\begin{aligned} \beta_v \nu \|\mathbf{w}_h\|_v^2 &\leq a_h(\mathbf{w}_h, \mathbf{w}_h) \\ &= a_h(\mathbf{u} - \mathbf{v}_h, \mathbf{w}_h) + a_h(\mathbf{u}_h - \mathbf{u}, \mathbf{w}_h) \\ &\leq C_a \nu \|\mathbf{u} - \mathbf{v}_h\|_v \|\mathbf{w}_h\|_v + a_h(\mathbf{u}_h, \mathbf{w}_h) - a_h(\mathbf{u}, \mathbf{w}_h) \\ &= C_a \nu \|\mathbf{u} - \mathbf{v}_h\|_v \|\mathbf{w}_h\|_v + \int_{\Omega} f \cdot \mathbf{w}_h \, dx - b_h(\mathbf{p}_h, \mathbf{w}_h) - a_h(\mathbf{u}, \mathbf{w}_h). \end{aligned} \quad (40)$$

The condition $b_h(\mathbf{q}_h, w_h) = 0 \forall \mathbf{q}_h \in X_h^q$ on w_h implies that $b_h(\mathbf{p}, w_h) = b_h(\mathbf{p}_h, w_h) = 0$, and with consistency (lemma 1) it also follows that $\int_{\Omega} f \cdot w_h \, dx - a_h(\mathbf{u}, \mathbf{w}_h) = 0$. Therefore, from eq. (40) we have $\|\|\mathbf{w}_h\|\|_v \leq (C_a/\beta_v)\|\|\mathbf{u} - \mathbf{v}_h\|\|_{v'}$ and

$$\|\|\mathbf{u} - \mathbf{u}_h\|\|_v \leq \|\|\mathbf{u} - \mathbf{v}_h\|\|_v + \|\|\mathbf{w}_h\|\|_v \leq \left(1 + \frac{C_a}{\beta_v}\right) \|\|\mathbf{u} - \mathbf{v}_h\|\|_{v'}. \quad (41)$$

This leads to

$$\|\|\mathbf{u} - \mathbf{u}_h\|\|_v \leq c \inf_{\substack{\mathbf{v}_h \in X_h^v \\ b_h(\mathbf{q}_h, \mathbf{v}_h) = 0 \forall \mathbf{q}_h \in X_h^q}} \|\|\mathbf{u} - \mathbf{v}_h\|\|_{v'} \leq Ch^k \|u\|_{k+1, \Omega}, \quad (42)$$

where the second inequality follows from setting $\mathbf{v}_h = \Pi \mathbf{u} = (\Pi_{\text{BDM}} u, \Pi_{L^2(\Gamma_0)} u)$, where $\Pi_{L^2(\Gamma_0)}$ is the L^2 -projection into the facet velocity space, and the application of the BDM interpolation in lemma 4 and standard polynomial interpolation and trace inequality estimates (see appendix Appendix A for the interpolation estimate). \square

The refined estimate shows that (i) the velocity error does not depend on the pressure, and as a consequence, (ii) the velocity error does not depend on the viscosity. Formulations in which the velocity error estimate is independent of the pressure are sometimes called *pressure robust* [26, 19].

Remark 1 (Lack of pressure robustness for the EDG case). For the EDG case, the analysis supporting theorem 2 breaks down due to the jump in the normal component of w_h not being zero across cell facets. If w_h is chosen to satisfy $b_h(\mathbf{q}_h, w_h) = 0 \forall \mathbf{q}_h \in X_h^q = Q_h \times \bar{Q}_h \cap C^0(\Gamma_0)$, eq. (40) holds but $b_h(\mathbf{p}, w_h) \neq 0$ and the step to eq. (41) breaks down. For the EDG case we have:

$$\begin{aligned} \beta_v \nu \|\|\mathbf{w}_h\|\|_v^2 &\leq C_a \nu \|\|\mathbf{u} - \mathbf{v}_h\|\|_{v'} \|\|\mathbf{w}_h\|\|_v + \int_{\Omega} f \cdot w_h \, dx - b_h(\mathbf{p}_h, w_h) - a_h(\mathbf{u}, \mathbf{w}_h) \\ &\leq C_a \nu \|\|\mathbf{u} - \mathbf{v}_h\|\|_{v'} \|\|\mathbf{w}_h\|\|_v + |b_h(\mathbf{p}, w_h)|. \end{aligned} \quad (43)$$

Since $b_h(\mathbf{p}, w_h) = b_h(\mathbf{p} - \mathbf{q}_h, w_h)$ as w_h is chosen such that $b_h(\mathbf{q}_h, w_h) = 0$, by boundedness of b_h ,

$$\|\|\mathbf{w}_h\|\|_v \leq \frac{C_a}{\beta} \|\|\mathbf{u} - \mathbf{v}_h\|\|_{v'} + \frac{1}{\beta_v \nu} \|\|\mathbf{p} - \mathbf{p}_h\|\|_p. \quad (44)$$

which leads to

$$\|\|\mathbf{u} - \mathbf{u}_h\|\|_v \leq c \inf_{\substack{\mathbf{v}_h \in X_h^v \\ b_h(\mathbf{q}_h, \mathbf{v}_h) = 0 \forall \mathbf{q}_h \in X_h^q}} \|\|\mathbf{u} - \mathbf{v}_h\|\|_{v'} + \frac{1}{\beta_v \nu} \inf_{\mathbf{q}_h \in X_h^q} \|\|\mathbf{p} - \mathbf{q}_h\|\|_p. \quad (45)$$

This shows for the EDG method that the velocity error has a dependence on $1/\nu$ times the pressure error. \square

By adjoint consistency of a_h and under appropriate regularity assumptions, for the HDG and EDG–HDG methods the error estimate

$$\|u - u_h\| \leq ch^{k+1} \|u\|_{k+1, \Omega} \quad (46)$$

follows straightforwardly from application of the Aubin–Nitsche trick. The analysis is included in appendix Appendix B for completeness.

4. Numerical tests

The performance of the three formulations is considered in terms of computed errors and solution time when solved using specially constructed preconditioned iterative solvers. Efficiency is also assessed in terms of the time required to compute solutions to a specific accuracy. An element is identified by the formulation type (HDG/EDG–HDG/EDG) and P^k – P^{k-1} , where the cell and facet velocity and facet pressure are approximated by polynomials of degree k , and the cell pressure is approximated by polynomials of degree $k - 1$. The penalty parameter is taken as $\alpha_v = 6k^2$ in 2D and $\alpha_v = 10k^2$ in 3D for HDG, and as $\alpha_v = 4k^2$ in 2D and $\alpha_v = 6k^2$ in 3D for EDG and EDG–HDG. The k -dependency is typical of interior penalty methods [36] and we find the constants to be reliable across a range of problems. All test cases have been implemented in MFEM [37] with solver support from PETSc [38, 39]. When applying algebraic multigrid, we use the BoomerAMG library [40].

4.1. Observed convergence rates

We consider the Kovasznay [41] problem on a domain $\Omega = (-0.5, 1) \times (-0.5, 1.5)$, for which the analytical solution is:

$$u_x = 1 - e^{\lambda x_1} \cos(2\pi x_2), \quad (47a)$$

$$u_y = \frac{\lambda}{2\pi} e^{\lambda x_1} \sin(2\pi x_2), \quad (47b)$$

$$p = \frac{1}{2} \left(1 - e^{2\lambda x_1} \right) + C, \quad (47c)$$

where C is an arbitrary constant, and where

$$\lambda = \frac{1}{2\nu} - \left(\frac{1}{4\nu^2} + 4\pi^2 \right)^{1/2}. \quad (48)$$

We choose C such that the mean pressure on Ω is zero. Dirichlet boundary conditions for the velocity on $\partial\Omega$ interpolate the analytical solution.

Observed rates of convergence for $\nu = 1/40$ are presented in table 1 for a series of refined meshes. Optimal rates of convergence are observed for all test cases, including for the remarkably simple P^1 – P^0 case.

4.2. Pressure robustness

Pressure robustness is demonstrated using the test case proposed in [19, Section 5.1]. On the domain $\Omega = (0, 1) \times (0, 1)$ we consider boundary conditions and a source term such that the exact solution is $u = \text{curl}\zeta$, where $\zeta = x_1^2(x_1 - 1)^2 x_2^2(x_2 - 1)^2$ and $p = x_1^5 + x_2^5 - 1/3$. We vary the viscosity ν and consider different orders of polynomial approximation. It can be observed in table 2 that the errors in the velocity for the HDG and EDG–HDG methods are indeed independent of the pressure and viscosity, as expected from theorem 2. The lack of pressure robustness for the EDG method is evident in table 2 where it is clear (in bold) that the velocity error increases as viscosity is decreased for the EDG method.

Table 1: Computed velocity, pressure and velocity divergence errors in the L^2 -norm, and rates of convergence, for the Kovaszny flow problem for the HDG, EDG and EDG–HDG methods for different orders of polynomial approximation.

HDG						
Degree	Cells	$\ u - u_h\ $	Order	$\ p - p_h\ $	Order	$\ \nabla \cdot u_h\ $
P^1-P^0	672	8.2e-3	1.9	4.2e-2	1.0	1.2e-14
	2,688	2.1e-3	2.0	2.1e-2	1.0	2.3e-14
	10,752	5.3e-4	2.0	1.1e-2	1.0	4.6e-14
	43,088	1.3e-4	2.0	5.4e-3	1.0	9.1e-14
P^2-P^1	672	7.1e-4	3.0	2.0e-3	1.9	5.6e-14
	2,688	8.7e-5	3.0	5.2e-4	1.9	1.6e-13
	10,752	1.1e-5	3.0	1.3e-4	2.0	2.0e-13
	43,088	1.3e-6	3.0	3.4e-5	2.0	4.3e-13
P^5-P^4	672	4.3e-8	6.0	1.9e-7	5.0	9.1e-13
	2,688	6.7e-10	6.0	6.0e-9	5.0	1.6e-12
	10,752	1.7e-11	5.3	1.9e-10	5.0	3.4e-12

EDG						
Degree	Cells	$\ u - u_h\ $	Order	$\ p - p_h\ $	Order	$\ \nabla \cdot u_h\ $
P^1-P^0	672	3.3e-2	1.8	4.3e-2	1.0	1.4e-14
	2,688	8.4e-3	2.0	2.1e-2	1.0	2.9e-14
	10,752	2.1e-3	2.0	1.1e-2	1.0	4.8e-14
	43,088	5.2e-4	2.0	5.2e-3	1.0	3.0e-13
P^2-P^1	672	9.0e-4	3.0	2.5e-3	1.8	5.0e-14
	2,688	1.1e-4	3.0	7.1e-4	1.8	9.9e-14
	10,752	1.4e-5	3.0	1.9e-4	1.9	1.9e-13
	43,088	1.7e-6	3.0	4.9e-5	2.0	3.8e-13
P^5-P^4	672	4.2e-8	6.0	1.6e-7	5.0	4.5e-13
	2,688	6.5e-10	6.0	5.0e-9	5.0	9.1e-13
	10,752	1.0e-11	6.0	1.5e-10	5.0	1.8e-12

EDG–HDG						
Degree	Cells	$\ u - u_h\ $	Order	$\ p - p_h\ $	Order	$\ \nabla \cdot u_h\ $
P^1-P^0	672	3.4e-2	1.9	4.4e-2	1.0	1.3e-14
	2,688	8.6e-3	2.0	2.2e-2	1.0	3.0e-14
	10,752	2.1e-3	2.0	1.1e-2	1.0	4.4e-14
	43,088	5.4e-4	2.0	5.4e-3	1.0	4.7e-13
P^2-P^1	672	9.4e-4	3.1	2.7e-3	1.8	5.2e-14
	2,688	1.2e-4	3.0	7.5e-4	1.9	9.3e-14
	10,752	1.4e-5	3.0	2.0e-4	1.9	1.9e-13
	43,088	1.7e-6	3.0	5.0e-5	2.0	4.3e-13
P^5-P^4	672	4.3e-8	6.0	1.69e-7	5.0	4.4e-13
	2,688	6.7e-10	6.0	5.23e-9	5.0	9.1e-13
	10,752	1.1e-11	6.0	1.62e-10	5.0	1.8e-12

Table 2: Computed velocity, pressure and velocity divergence errors in the L^2 -norm for the pressure robustness test case for the HDG (H), EDG (E) and EDG–HDG (EH) methods for different orders of polynomial approximation. H-10 represents an HDG P^1 – P^0 discretization, etc.

Cells	Method	$\nu = 1$			$\nu = 10^{-6}$		
		$\ u - u_h\ $	$\ p - p_h\ $	$\ \nabla \cdot u_h\ $	$\ u - u_h\ $	$\ p - p_h\ $	$\ \nabla \cdot u_h\ $
131,072	H-10	5.0e-7	2.4e-3	1.1e-15	5.0e-7	2.4e-3	7.6e-11
131,072	E-10	9.2e-7	2.4e-3	1.0e-15	4.8e-3	2.4e-3	1.1e-10
131,072	EH-10	1.1e-6	2.4e-3	1.1e-15	1.1e-6	2.4e-3	0.8e-11
2,048	H-21	4.7e-7	4.3e-4	6.0e-16	5.2e-7	3.2e-4	5.4e-11
2,048	E-21	6.8e-7	5.2e-4	1.6e-15	4.6e-3	3.2e-4	6.4e-11
2,048	EH-21	7.0e-7	5.3e-4	5.6e-16	7.4e-7	3.2e-4	6.6e-11
128	H-43	2.6e-7	3.9e-5	1.8e-15	2.6e-7	3.8e-6	1.0e-10
128	E-43	2.7e-7	3.7e-5	1.7e-15	3.0e-5	3.8e-6	1.2e-10
128	EH-43	2.7e-7	3.7e-5	1.7e-15	2.7e-7	3.8e-6	1.1e-10

4.3. Minimal regularity test

We consider the Stokes problem on the L-shaped domain $\Omega := (-1, 1)^2 \setminus [-1, 0] \times [0, 1]$ with $\nu = 1$ and $f = 0$, see, e.g. [42, 43]. The Dirichlet boundary data are interpolated from the exact solution, which in polar coordinates is given by:

$$u_x = r^\lambda [(1 + \alpha) \sin(\varphi) \psi(\varphi) + \cos(\varphi) \partial_\varphi \psi(\varphi)] \quad (49a)$$

$$u_y = r^\lambda [-(1 + \alpha) \cos(\varphi) \psi(\varphi) + \sin(\varphi) \partial_\varphi \psi(\varphi)] \quad (49b)$$

$$p = -r^{\lambda-1} [(1 + \lambda)^2 \partial_\varphi \psi(\varphi) + \partial_\varphi^3 \psi(\varphi)] / (1 - \lambda), \quad (49c)$$

where

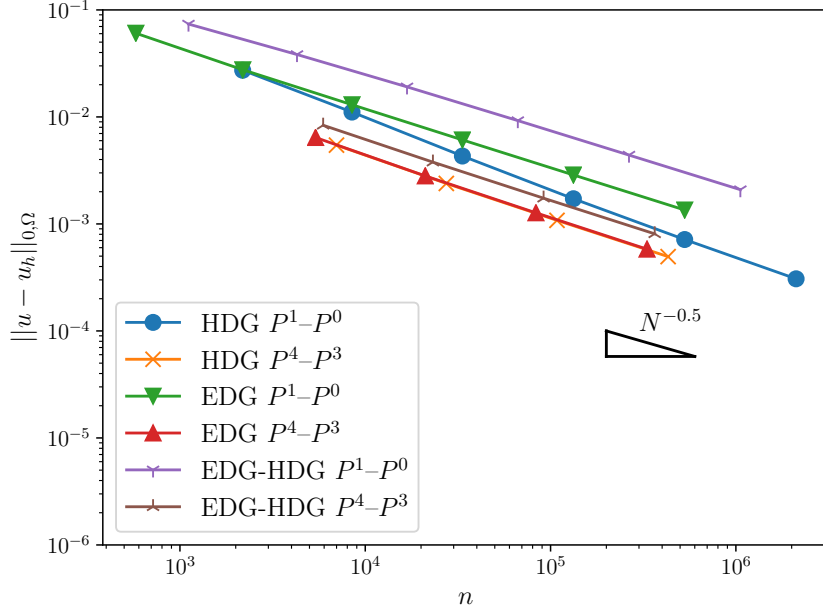
$$\begin{aligned} \psi(\varphi) = & \sin((1 + \lambda)\varphi) \cos(\lambda\omega) / (1 + \lambda) - \cos((1 + \lambda)\varphi) \\ & - \sin((1 - \lambda)\varphi) \cos(\lambda\omega) / (1 - \lambda) + \cos((1 - \lambda)\varphi), \end{aligned} \quad (50)$$

and where $\omega = 3\pi/2$ and $\lambda \approx 0.54448373678246$. Note that $u \notin [H^2(\Omega)]^2$ and $p \notin H^1(\Omega)$ for this problem.

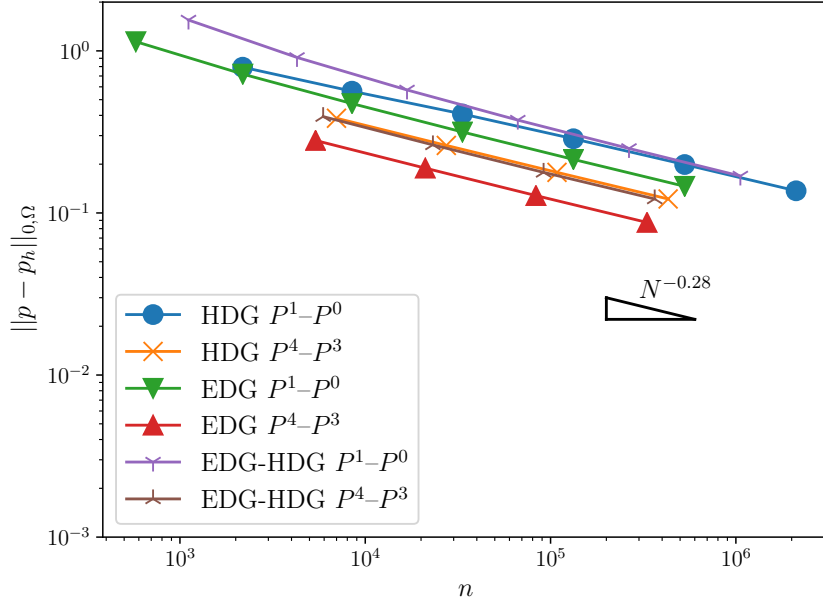
Figure 1 presents the computed velocity and pressure errors for P^1 – P^0 and P^4 – P^3 discretizations against the total number of degrees-of-freedom. The solutions are observed to converge, and the velocity and pressure errors are approximately of order $\mathcal{O}(h)$ and $\mathcal{O}(h^{1/2})$, respectively. This is an example where use of the very simple P^1 – P^0 discretization could be appealing.

4.4. Preconditioned linear solvers

A motivation for considering EDG–HDG and EDG methods is efficiency when combined with preconditioned iterative solvers, and in particular the similarity of EDG–HDG and EDG to continuous methods for which a range of solvers are known to perform well. In [29] we introduced an optimal preconditioner for the statically condensed (cell-wise velocity eliminated locally) linear system obtained from the HDG discretization of the Stokes problem, and the analysis holds also



(a) Velocity error.



(b) Pressure error.

Figure 1: Computed velocity and pressure errors in the L^2 -norm versus total number of degrees-of-freedom (n) for the minimal regularity solution test case.

for the EDG and EDG–HDG methods. The preconditioner is presented here and we refer to [29] for the analysis.

The discrete problem for eq. (15) has the form:

$$\begin{bmatrix} A_{uu} & \mathbf{B}^T \\ \mathbf{B} & \mathbf{C} \end{bmatrix} \begin{bmatrix} u \\ \mathbf{U} \end{bmatrix} = \begin{bmatrix} L_u \\ \mathbf{L} \end{bmatrix}, \quad \mathbf{U} := \begin{bmatrix} \bar{u} \\ p \\ \bar{p} \end{bmatrix}, \quad \mathbf{L} := \begin{bmatrix} L_{\bar{u}} \\ 0 \\ 0 \end{bmatrix}, \quad (51)$$

with

$$\mathbf{B} := \begin{bmatrix} A_{\bar{u}u} \\ B_{pu} \\ B_{\bar{p}u} \end{bmatrix}, \quad \mathbf{C} := \begin{bmatrix} A_{\bar{u}\bar{u}} & 0 & 0 \\ 0 & 0 & 0 \\ 0 & 0 & 0 \end{bmatrix}. \quad (52)$$

Here $u \in \mathbb{R}^{n_u}$ and $\bar{u} \in \mathbb{R}^{\bar{n}_u}$ are the vectors of the discrete velocity with respect to the basis for the cell-wise and facet velocities, respectively, and $p \in \mathbb{R}^{n_p}$ and $\bar{p} \in \mathbb{R}^{\bar{n}_p}$ are the vectors of the discrete pressure with respect to the basis for the cell-wise and facet pressures, respectively. Furthermore, A_{uu} , $A_{\bar{u}u}$ and $A_{\bar{u}\bar{u}}$ are the matrices obtained from the discretization of $a_h((\cdot, 0), (\cdot, 0))$, $a_h((\cdot, 0), (0, \cdot))$ and $a_h((0, \cdot), (0, \cdot))$, respectively, and B_{pu} and $B_{\bar{p}u}$ are the matrices obtained from the discretization of $b_h((\cdot, 0), (\cdot, 0))$ and $b_h((0, \cdot), (\cdot, 0))$. Noting that A_{uu} is a block diagonal matrix (one block per cell), it is possible to efficiently eliminate u from eq. (51) using $u = A_{uu}^{-1} (L_u - \mathbf{B}^T \mathbf{U})$. This results in a reduced system for \mathbf{U} only,

$$\begin{bmatrix} -A_{\bar{u}u}A_{uu}^{-1}A_{\bar{u}u}^T + A_{\bar{u}\bar{u}} & -A_{\bar{u}u}A_{uu}^{-1}B_{pu}^T & -A_{\bar{u}u}A_{uu}^{-1}B_{\bar{p}u} \\ -B_{pu}A_{uu}^{-1}A_{\bar{u}u}^T & -B_{pu}A_{uu}^{-1}B_{pu}^T & -B_{pu}A_{uu}^{-1}B_{\bar{p}u}^T \\ -B_{\bar{p}u}A_{uu}^{-1}A_{\bar{u}u}^T & -B_{\bar{p}u}A_{uu}^{-1}B_{pu}^T & -B_{\bar{p}u}A_{uu}^{-1}B_{\bar{p}u}^T \end{bmatrix} \begin{bmatrix} \bar{u} \\ p \\ \bar{p} \end{bmatrix} = \begin{bmatrix} L_{\bar{u}} - A_{\bar{u}u}A_{uu}^{-1}L_u \\ -B_{pu}A_{uu}^{-1}L_u \\ -B_{\bar{p}u}A_{uu}^{-1}L_u \end{bmatrix}. \quad (53)$$

In [29] we introduced three optimal preconditioners for the reduced form of the hybrid discretizations of the Stokes problem: two block diagonal preconditioners and a block symmetric Gauss–Seidel preconditioner. We discuss here only the block symmetric Gauss–Seidel preconditioner. Let \mathcal{P}_D and \mathcal{P}_L be, respectively, the block-diagonal and the strictly lower triangular part of the system matrix in eq. (53). The block symmetric Gauss–Seidel preconditioner is then given by

$$\mathcal{P} = (\mathcal{P}_L + \mathcal{P}_D)\mathcal{P}_D^{-1}(\mathcal{P}_L^T + \mathcal{P}_D). \quad (54)$$

As discussed in [29], algebraic multigrid can successfully be applied to approximate the inverse of \mathcal{P}_D .

Optimality of the preconditioner in eq. (54) for the HDG, EDG–HDG and EDG methods is tested for P^1 – P^0 and P^2 – P^1 polynomial approximations. In all cases we use MINRES for the outer iterations, with AMG (four multigrid V-cycles) to approximate the inverse of each block of \mathcal{P}_D . In all cases, the solver is terminated once the relative true residual reaches a tolerance of 10^{-12} .

We consider lid-driven cavity flow in the unit square $\Omega = [-1, 1]^2$ and a cube $\Omega = [0, 1]^3$, using unstructured simplicial meshes. Dirichlet boundary conditions are imposed on $\partial\Omega$. In two dimensions, $u = (1 - x_1^4, 0)$ on the boundary $x_2 = 1$ and the zero velocity vector on remaining boundaries. In three dimensions we impose $u = (1 - \tau_1^4, \frac{1}{10}(1 - \tau_2^4), 0)$, with $\tau_i = 2x_i - 1$, on the boundary $x_3 = 1$ and the zero velocity vector on remaining boundaries. We set $\nu = 1$. Table 3 presents the number of iterations for the two-dimensional problem and table 4 presents the number of iterations for the three-dimensional problem. The preconditioner in eq. (54) is observed to be

Table 3: Iteration counts for preconditioned MINRES for the relative true residual to reach a tolerance of 10^{-12} for the lid-driven cavity problem in two dimensions.

P^1-P^0						
Cells	HDG		EDG		EDG–HDG	
	DOFs	Its	DOFs	Its	DOFs	Its
176	1,892	204	509	177	970	193
704	7,304	217	1,895	194	3,698	211
2,816	28,688	230	7,307	200	14,434	212
11,264	113,696	234	28,691	191	57,026	198
45,056	452,672	236	113,699	193	226,690	197
P^2-P^1						
Cells	HDG		EDG		EDG–HDG	
	DOFs	Its	DOFs	Its	DOFs	Its
176	3,102	156	1,719	129	2,180	129
704	12,012	166	6,603	131	8,406	131
2,816	47,256	170	25,875	132	33,002	131
11,264	187,440	182	102,435	130	130,770	129
45,056	746,592	184	407,619	127	520,610	126

optimal for all methods in both two and three dimensions – the iteration count is independent of the problem size, or at worst exhibits a weak growth with increasing problem size. In all cases the solver converges in fewer iterations for the EDG and EDG–HDG methods compared to the HDG method. For example, on the finest grid in three dimensions, using a P^2-P^1 discretization, HDG requires 300 iterations to converge, compared to 132 for EDG and 151 for EDG–HDG.

4.5. Performance comparison

We compare the overall performance of the HDG, EDG–HDG and EDG methods in terms of solution time for a given level of accuracy using a problem with $\nu = 1$ on the unit cube $\Omega = [0, 1]^3$ with source and Dirichlet boundary conditions such that the exact solution is given by

$$u = \pi \begin{bmatrix} \sin(\pi x_1) \cos(\pi x_2) - \sin(\pi x_1) \cos(\pi x_3) \\ \sin(\pi x_2) \cos(\pi x_3) - \sin(\pi x_2) \cos(\pi x_1) \\ \sin(\pi x_3) \cos(\pi x_1) - \sin(\pi x_3) \cos(\pi x_2) \end{bmatrix}, \quad p = \sin(\pi x) \sin(\pi y) \sin(\pi z) - 8/\pi^3. \quad (55)$$

Meshes are composed of unstructured tetrahedral cells and generated using Gmsh. We apply GMRES with restarts after 30 iterations, with the preconditioner in section 4.4 applied. The iterative method is terminated once the relative true residual reaches 10^{-12} .

The performance results for P^2-P^1 and P^3-P^2 discretizations are presented in table 5. We observe that the velocity error is approximately 1.2–1.6 times higher for the EDG–HDG and EDG methods when compared to the HDG method on the same mesh. However, the time to compute the solution using the EDG–HDG or EDG method is substantially lower compared to the HDG discretization. This is due to the global linear systems for the EDG–HDG and EDG methods being significantly smaller for a given mesh, and the systems solving in fewer iterations. Particularly noteworthy is the P^2-P^1 EDG simulation on the finest mesh, for which compared to the P^2-P^1 HDG solution the error is 1.4 times greater in the L_2 -norm but the solution time is just 1/20th.

Table 4: Iteration counts for preconditioned MINRES for the relative true residual to reach a tolerance of 10^{-12} for the lid-driven cavity problem in three dimensions.

P^1-P^0						
Cells	HDG		EDG		EDG-HDG	
	DOFs	Its	DOFs	Its	DOFs	Its
524	14,540	258	1,180	169	4,520	190
4,192	110,560	302	8,076	189	33,697	218
33,536	861,440	327	59,988	189	260,351	210
P^2-P^1						
Cells	HDG		EDG		EDG-HDG	
	DOFs	Its	DOFs	Its	DOFs	Its
524	30,128	227	5,980	136	12,017	151
4,192	229,504	265	43,220	136	89,791	161
33,536	1,789,952	300	328,868	132	694,139	151

Table 5: Results are normalized with respect to the results of HDG on each mesh (in brackets). Here n is the total number of degrees of freedom of the global system after static condensation.

P^2-P^1					
Mesh	Method	Rel. $\ u - u_h\ $	Rel. n	Rel. its	Rel. time
1 (524 cells)	HDG	1 (2.0e-2)	1 (30 128)	1 (51)	1 (7.5 s)
	EDG-HDG	1.59	0.4	0.88	0.27
	EDG	1.49	0.2	0.80	0.12
2 (4192 cells)	HDG	1 (4.8e-3)	1 (229 504)	1 (55)	1 (79 s)
	EDG-HDG	1.58	0.4	0.76	0.12
	EDG	1.45	0.2	0.65	0.08
3 (33 536 cells)	HDG	1 (1.0e-3)	1 (1 789 953)	1 (58)	1 (770 s)
	EDG-HDG	1.51	0.4	0.55	0.09
	EDG	1.38	0.2	0.52	0.06
P^3-P^2					
Mesh	Method	Rel. $\ u - u_h\ $	Rel. n	Rel. its	Rel. time
1 (524 cells)	HDG	1 (1.4e-3)	1 (51 960)	1 (64)	1 (22 s)
	EDG-HDG	1.38	0.5	0.72	0.17
	EDG	1.30	0.3	0.67	0.13
2 (4192 cells)	HDG	1 (2.6e-4)	1 (396 480)	1 (68)	1 (s)
	EDG-HDG	1.52	0.5	0.59	0.13
	EDG	1.20	0.3	0.57	0.10
3 (33 536 cells)	HDG	1 (3.2e-5)	1 (3 095 040)	1 (69)	1 (2105 s)
	EDG-HDG	1.23	0.5	0.51	0.14
	EDG	1.15	0.3	0.49	0.11

5. Conclusions

We have introduced and analyzed a new embedded–hybridized discontinuous Galerkin (EDG–HDG) finite element method for the Stokes problem. The analysis is unified in that it also covers the previously presented hybridized (HDG) and embedded discontinuous Galerkin (EDG) methods for the Stokes problem. All three methods are stable, have optimal rates of convergence and satisfy the continuity equation pointwise. Only the HDG and the EDG–HDG methods have velocity fields that are $H(\text{div})$ -conforming, and it is proved that a consequence of this is that velocity error estimates are independent of the pressure. The analysis results are supported by numerical experiments. Noteworthy is that the analysis holds for the extremely simple piecewise linear/constant pair for velocity/pressure field. The work was motivated by the question of whether the EDG–HDG method could preserve the attractive features of the HDG formulation and be more amenable to fast iterative solvers. This has been shown to be the case, supported by analysis and numerical examples. Numerical examples demonstrate optimality of a carefully constructed preconditioner, and for a given accuracy the EDG–HDG method is considerably faster than the HDG method.

Acknowledgements

SR gratefully acknowledges support from the Natural Sciences and Engineering Research Council of Canada through the Discovery Grant program (RGPIN-05606-2015) and the Discovery Accelerator Supplement (RGPAS-478018-2015).

Appendix A. Interpolation estimate

Lemma 9. For $v \in [H^1(\Omega)]^d$, let $\Pi \mathbf{v} = (\Pi_{\text{BDM}} v, \Pi_{L^2(\Gamma_0)} v)$ where Π_{BDM} is the BDM interpolation operator in lemma 4, and $\Pi_{L^2(\Gamma_0)}$ is the L^2 -projection into \tilde{V}_h . Then

$$\|\mathbf{v} - \Pi \mathbf{v}\|_{v'} \leq ch^k \|v\|_{k+1, \Omega}. \quad (\text{A.1})$$

PROOF. By definition,

$$\begin{aligned} \|\mathbf{v} - \Pi \mathbf{v}\|_{v'}^2 &= \sum_{K \in \mathcal{T}} \|\nabla(v - \Pi_{\text{BDM}} v)\|_K^2 + \sum_{K \in \mathcal{T}} \frac{\alpha_v}{h_K} \|\Pi_{\text{BDM}} v - \Pi_{L^2(\Gamma_0)} v\|_{\partial K}^2 \\ &\quad + \sum_{K \in \mathcal{T}} \frac{h_K}{\alpha_v} \|\nabla(v - \Pi_{\text{BDM}} v) \cdot n\|_{\partial K}^2. \end{aligned} \quad (\text{A.2})$$

We will bound each term on the right-hand side of eq. (A.2) separately.

By lemma 4 item ii,

$$\sum_{K \in \mathcal{T}} \|\nabla(v - \Pi_{\text{BDM}} v)\|_K^2 \leq ch^{2k} \|v\|_{k+1, \Omega}^2. \quad (\text{A.3})$$

By the triangle inequality

$$\begin{aligned} \sum_{K \in \mathcal{T}} \frac{\alpha_v}{h_K} \|\Pi_{\text{BDM}} v - \Pi_{L^2(\Gamma_0)} v\|_{\partial K}^2 \\ \leq \sum_{K \in \mathcal{T}} \frac{\alpha_v}{h_K} \|\Pi_{\text{BDM}} v - v\|_{\partial K}^2 + \sum_{K \in \mathcal{T}} \frac{\alpha_v}{h_K} \|v - \Pi_{L^2(\Gamma_0)} v\|_{\partial K}^2. \end{aligned} \quad (\text{A.4})$$

Applying a continuous trace inequality to the first term on the right hand side of eq. (A.4), and by lemma 4 item ii,

$$\begin{aligned} \sum_{K \in \mathcal{T}} \frac{\alpha_v}{h_K} \|\Pi_{\text{BDM}} v - v\|_{\partial K}^2 &\leq c \sum_{K \in \mathcal{T}} \left(h_K^{-2} \|\Pi_{\text{BDM}} v - v\|_K^2 + |\Pi_{\text{BDM}} v - v|_{1,K}^2 \right) \\ &\leq ch^{2k} \|v\|_{k+1,\Omega}^2. \end{aligned} \quad (\text{A.5})$$

Similarly, applying a continuous trace inequality to the second term on the right-hand side of eq. (A.4), and properties of the L^2 -projection operator (e.g. [30]),

$$\begin{aligned} \sum_{K \in \mathcal{T}} \frac{\alpha_v}{h_K} \|\Pi_{L^2(\Gamma_0)} v - v\|_{\partial K}^2 &\leq c \sum_{K \in \mathcal{T}} \left(h_K^{-2} \|\Pi_{L^2(\Gamma_0)} v - v\|_K^2 + |\Pi_{L^2(\Gamma_0)} v - v|_{1,K}^2 \right) \\ &\leq ch^{2k} \|v\|_{k+1,\Omega}^2. \end{aligned} \quad (\text{A.6})$$

Finally, by a continuous trace inequality and lemma 4 item ii,

$$\begin{aligned} \sum_{K \in \mathcal{T}} \frac{h_K}{\alpha_v} \|\nabla(v - \Pi_{\text{BDM}} v) \cdot n\|_{\partial K}^2 &\leq \sum_{K \in \mathcal{T}} c \left(|v - \Pi_{\text{BDM}} v|_{1,K}^2 + h_K^2 |v - \Pi_{\text{BDM}} v|_{2,K}^2 \right) \\ &\leq ch^{2k} \|v\|_{k+1,\Omega}^2. \end{aligned} \quad (\text{A.7})$$

The result follows by combining the bounds for each term in eq. (A.2). \square

Appendix B. Pressure-robust L^2 error estimate

Following the steps to prove theorem 2 and exploiting equivalence of the $\|\cdot\|_v$ and $\|\cdot\|_{v'}$ norms on $V_h \times \bar{V}_h$ leads to the following:

Corollary 1 (Approximation in the $\|\cdot\|_{v'}$ norm). *Let $u \in [H^{k+1}(\Omega)]^d$ be the velocity solution of the Stokes problem eq. (1) with $k \geq 1$, let $\mathbf{u} = (u, u)$, and let $\mathbf{u}_h \in X_h^v$ be the velocity solution of the finite element problem eq. (15) for the HDG or EDG-HDG formulations. Then*

$$\|\mathbf{u} - \mathbf{u}_h\|_{v'} \leq ch^k \|u\|_{k+1,\Omega}. \quad (\text{B.1})$$

To prove a velocity error estimate in the L^2 -norm we will rely on the following regularity assumption. If (u, p) solves the Stokes problem eq. (1) for $f \in [L^2(\Omega)]^d$, we have on a convex polygonal domain

$$\nu \|u\|_{2,\Omega} + \|p\|_{1,\Omega} \leq c_r \|f\|_{\Omega}, \quad (\text{B.2})$$

where c_r is a constant [44, Chapter II].

Lemma 10 (Boundedness of a_h on the extended space). *There exists a $C_a > 0$, independent of h , such that for all $\mathbf{u} \in V(h) \times \bar{V}(h)$ and for all $\mathbf{v} \in V(h) \times \bar{V}(h)$*

$$|a_h(\mathbf{u}, \mathbf{v})| \leq C_a \nu \|\mathbf{u}\|_{v'} \|\mathbf{v}\|_{v'}. \quad (\text{B.3})$$

The proof of this is identical to that for [5, Lemma 4.3].

Theorem 3 (Pressure robust velocity error estimate in the L^2 -norm). *Let $(u, p) \in [H^{k+1}(\Omega)]^d \times H^k(\Omega)$ solve the Stokes problem eq. (1) with $k \geq 1$, and let $\mathbf{u} = (u, u)$ and $\mathbf{p} = (p, p)$. If $(\mathbf{u}_h, \mathbf{p}_h) \in X_h$ solves the finite element problem eq. (15) for the HDG or EDG–HDG formulation then, subject to the regularity condition in eq. (B.2), there exists a constant $C_V > 0$, independent of h , such that*

$$\|u - u_h\|_{\Omega} \leq C_V h^{k+1} \|u\|_{k+1, \Omega}. \quad (\text{B.4})$$

PROOF. Let $(\zeta_u, \zeta_p) \in X$ solve the Stokes problem eq. (1) for $f = (u - u_h)$. Then

$$a_h((\zeta_u, \zeta_u), \mathbf{v}) + b_h((\zeta_p, \zeta_p), v) = \int_{\Omega} (u - u_h) \cdot v \, dx \quad \forall \mathbf{v} \in V(h) \times \bar{V}(h). \quad (\text{B.5})$$

Setting $\mathbf{v} = \mathbf{u} - \mathbf{u}_h$ and noting that $b_h((\zeta_p, \zeta_p), v) = 0$ by the regularity of ζ_p and by v being divergence-free and $H(\text{div})$ -conforming, we have

$$a_h((\zeta_u, \zeta_u), \mathbf{u} - \mathbf{u}_h) = \|u - u_h\|_{\Omega}^2. \quad (\text{B.6})$$

Note also that

$$a_h(\mathbf{v}_h, \mathbf{u} - \mathbf{u}_h) = 0 \quad \forall \mathbf{v}_h \in X_h^v \quad (\text{B.7})$$

by adjoint consistency. Setting $\mathbf{v}_h = \Pi \zeta_u$ where Π is the projection in lemma 9, then by boundedness of a_h eq. (B.3),

$$\begin{aligned} \|u - u_h\|_{\Omega}^2 &= a_h(\zeta_u - \Pi \zeta_u, \mathbf{u} - \mathbf{u}_h) \\ &\leq C\nu \|\zeta_u - \Pi \zeta_u\|_{v'} \|\mathbf{u} - \mathbf{u}_h\|_{v'} \\ &\leq C\nu h \|\zeta_u\|_2 \|\mathbf{u} - \mathbf{u}_h\|_{v'} \\ &\leq Ch \|u - u_h\| \|\mathbf{u} - \mathbf{u}_h\|_{v'}, \end{aligned} \quad (\text{B.8})$$

hence

$$\|u - u_h\|_{\Omega} \leq Ch \|\mathbf{u} - \mathbf{u}_h\|_{v'}. \quad (\text{B.9})$$

The result follows from applying corollary 1 to $\|\mathbf{u} - \mathbf{u}_h\|_{v'}$. \square

References

- [1] B. Cockburn, J. Gopalakrishnan, The derivation of hybridizable discontinuous Galerkin methods for Stokes flow, *SIAM J. Numer. Anal.* 47 (2009) 1092–1125. URL: <https://doi.org/10.1137/080726653>.
- [2] B. Cockburn, J. Gopalakrishnan, N. C. Nguyen, J. Peraire, F. J. Sayas, Analysis of HDG methods for Stokes flow, *Math. Comp.* 80 (2011) 723–760. URL: <http://dx.doi.org/10.1090/S0025-5718-2010-02410-X>.
- [3] B. Cockburn, F.-J. Sayas, Divergence-conforming HDG methods for Stokes flows, *Math. Comp.* 83 (2014) 1571–1598. URL: <https://doi.org/10.1090/S0025-5718-2014-02802-0>.
- [4] N. C. Nguyen, J. Peraire, B. Cockburn, A hybridizable discontinuous Galerkin method for Stokes flow, *Comput. Methods Appl. Mech. Engrg.* 199 (2010) 582–597. URL: <http://dx.doi.org/10.1016/j.cma.2009.10.007>.
- [5] S. Rhebergen, G. N. Wells, Analysis of a hybridized/interface stabilized finite element method for the Stokes equations, *SIAM J. Numer. Anal.* 55 (2017) 1982–2003. URL: <http://doi.org/10.1137/16M1083839>.
- [6] S. Güzey, B. Cockburn, H. Stolarski, The embedded discontinuous Galerkin methods: Application to linear shells problems, *Int. J. Numer. Methods Engrg.* 70 (2007) 757–790. URL: <https://doi.org/10.1002/nme.1893>.
- [7] R. J. Labeur, G. N. Wells, A Galerkin interface stabilisation method for the advection–diffusion and incompressible Navier–Stokes equations, *Comput. Methods Appl. Mech. Engrg.* 196 (2007) 4985–5000. URL: <http://dx.doi.org/10.1016/j.cma.2007.06.025>.

- [8] R. J. Labeur, G. N. Wells, Energy stable and momentum conserving hybrid finite element method for the incompressible Navier–Stokes equations, *SIAM J Sci Comput* 34 (2012) A889–A913. URL: <http://dx.doi.org/10.1137/100818583>.
- [9] D. Boffi, F. Brezzi, M. Fortin, *Mixed Finite Element Methods and Applications*, volume 44 of *Springer Series in Computational Mathematics*, Springer–Verlag Berlin Heidelberg, 2013.
- [10] C. Lehrenfeld, Hybrid discontinuous Galerkin methods for solving incompressible flow problems, Master’s thesis, Rheinisch-Westfälischen Technischen Hochschule Aachen, 2010. URL: https://www.igpm.rwth-aachen.de/Download/reports/lehrenfeld/DA_HDG4NSE_1_0.pdf.
- [11] C. Lehrenfeld, J. Schöberl, High order exactly divergence-free hybrid discontinuous Galerkin methods for unsteady incompressible flows, *Comput. Methods Appl. Mech. Engrg.* 307 (2016) 339–361. URL: <http://dx.doi.org/10.1016/j.cma.2016.04.025>.
- [12] A. Cesmelioglu, B. Cockburn, N. C. Nguyen, J. Peraire, Analysis of HDG methods for Oseen equations, *J. Sci. Comput.* 55 (2013) 392–431. URL: <https://doi.org/10.1007/s10915-012-9639-y>.
- [13] B. Cockburn, G. Kanschat, D. Schötzau, C. Schwab, Local discontinuous Galerkin methods for the Stokes system, *SIAM J. Numer. Anal.* 40 (2002) 319–343. URL: <http://dx.doi.org/10.1137/S0036142900380121>.
- [14] B. Cockburn, G. Kanschat, D. Schötzau, The local discontinuous Galerkin method for the Oseen equations, *Math. Comp.* 73 (2003) 569–593. URL: <http://dx.doi.org/10.1090/S0025-5718-03-01552-7>.
- [15] B. Cockburn, G. Kanschat, D. Schötzau, A locally conservative LDG method for the incompressible Navier–Stokes equations, *Math. Comp.* 74 (2004) 1067–1095. URL: <https://doi.org/10.1090/S0025-5718-04-01718-1>.
- [16] B. Cockburn, G. Kanschat, D. Schötzau, A note on discontinuous Galerkin divergence-free solutions of the Navier–Stokes equations, *J. Sci. Comput.* 31 (2007) 61–73. URL: <https://doi.org/10.1007/s10915-006-9107-7>.
- [17] J. Wang, X. Ye, New finite element methods in computational fluid dynamics by H(div) elements, *SIAM J. Numer. Anal.* 45 (2007) 1269–1286. URL: <https://doi.org/10.1137/060649227>.
- [18] G. Fu, An explicit divergence-free DG method for incompressible flow, *Comput. Methods Appl. Mech. Engrg.* 345 (2019) 502–517. URL: <https://doi.org/10.1016/j.cma.2018.11.012>.
- [19] P. L. Lederer, C. Lehrenfeld, J. Schöberl, Hybrid discontinuous Galerkin methods with relaxed H(div)-conformity for incompressible flows. Part I, *SIAM J. Numer. Anal.* 56 (2018) 2070–2094. URL: <https://doi.org/10.1137/17M1138078>.
- [20] S. Rhebergen, G. N. Wells, A hybridizable discontinuous Galerkin method for the Navier–Stokes equations with pointwise divergence-free velocity field, *J. Sci. Comput.* 76 (2018) 1484–1501. URL: <https://doi.org/10.1007/s10915-018-0671-4>.
- [21] C. Brennecke, A. Linke, C. Merdon, J. Schöberl, Optimal and pressure-independent L^2 velocity error estimates for a modified Crouzeix–Raviart Stokes element with BDM reconstructions, *J. Comput. Math.* 33 (2015) 191–208. URL: <http://dx.doi.org/10.4208/jcm.1411-m4499>.
- [22] P. L. Lederer, A. Linke, C. Merdon, J. Schöberl, Divergence-free reconstruction operators for pressure-robust Stokes discretizations with continuous pressure finite elements, *SIAM J. Numer. Anal.* 55 (2017) 1291–1314. URL: <https://doi.org/10.1137/16M1089964>.
- [23] A. Linke, C. Merdon, On velocity errors due to irrotational forces in the Navier–Stokes momentum balance, *J. Comput. Phys.* 313 (2016) 654–661. URL: <http://dx.doi.org/10.1016/j.jcp.2016.02.070>.
- [24] A. Linke, C. Merdon, Pressure-robustness and discrete Helmholtz projectors in mixed finite element methods for the incompressible Navier–Stokes equations, *Comput. Methods Appl. Mech. Engrg.* (2016). URL: <http://dx.doi.org/10.1016/j.cma.2016.08.018>.
- [25] P. Schroeder, G. Lube, Divergence-free H(div)-fem for time-dependent incompressible flows with applications to high Reynolds number vortex dynamics, *J. Sci. Comput.* 75 (2018) 830–858. URL: <https://doi.org/10.1007/s10915-017-0561-1>.
- [26] V. John, A. Linke, C. Merdon, M. Neilan, L. G. Rebholz, On the divergence constraint in mixed finite element methods for incompressible flows, *SIAM Rev.* 59 (2017) 492–544. URL: <http://doi.org/10.1137/15M1047696>.
- [27] J. Guzmán, C.-W. Shu, F. Sequeira, H(div) conforming and DG methods for incompressible Euler’s equations, *IMA Journal of Numerical Analysis* 37 (2016) 1733–1771. URL: <https://doi.org/10.1093/imanum/drw054>.
- [28] B. Cockburn, J. Guzmán, S.-C. Soen, H. K. Stolarski, An analysis of the embedded discontinuous Galerkin method for second-order elliptic problems, *SIAM J. Numer. Anal.* 47 (2009) 2686–2707. URL: <http://dx.doi.org/10.1137/080726914>.
- [29] S. Rhebergen, G. N. Wells, Preconditioning of a hybridized discontinuous Galerkin finite element method for the Stokes equations, *J. Sci. Comput.* 77 (2018) 1936–1952. URL: <https://doi.org/10.1007/s10915-018-0760-4>.

- [30] D. A. Di Pietro, A. Ern, *Mathematical Aspects of Discontinuous Galerkin Methods*, volume 69 of *Mathématiques et Applications*, Springer–Verlag Berlin Heidelberg, 2012.
- [31] G. N. Wells, Analysis of an interface stabilized finite element method: the advection-diffusion-reaction equation, *SIAM J. Numer. Anal.* 49 (2011) 87–109. URL: <http://dx.doi.org/10.1137/090775464>.
- [32] P. Hansbo, M. G. Larson, Discontinuous Galerkin methods for incompressible and nearly incompressible elasticity by Nitsche’s method, *Comput. Methods Appl. Mech. Engrg.* 191 (2002) 1895–1908. URL: [http://dx.doi.org/10.1016/S0045-7825\(01\)00358-9](http://dx.doi.org/10.1016/S0045-7825(01)00358-9).
- [33] S. C. Brenner, L. R. Scott, *The Mathematical Theory of Finite Element Methods*, 3rd ed., Springer, 2010.
- [34] J. S. Howell, N. J. Walkington, Inf-sup conditions for twofold saddle point problems, *Numer. Math.* 118 (2011) 663–693. URL: <http://dx.doi.org/10.1007/s00211-011-0372-5>.
- [35] G. N. Gatica, *A Simple Introduction to the Mixed Finite Element Method*, Springer Briefs in Mathematics, Springer, 2014.
- [36] B. Rivière, *Discontinuous Galerkin Methods for Solving Elliptic and Parabolic Equations*, volume 35 of *Frontiers in Applied Mathematics*, Society for Industrial and Applied Mathematics, Philadelphia, 2008.
- [37] V. A. Dobrev, T. V. Kolev, et al., *MFEM: Modular finite element methods*, 2018. URL: <http://mfem.org>.
- [38] S. Balay, S. Abhyankar, M. F. Adams, J. Brown, P. Brune, K. Buschelman, L. Dalcin, V. Eijkhout, W. D. Gropp, D. Kaushik, M. G. Knepley, L. C. McInnes, K. Rupp, B. F. Smith, S. Zampini, H. Zhang, H. Zhang, *PETSc Users Manual*, Technical Report ANL-95/11 - Revision 3.7, Argonne National Laboratory, 2016. URL: <http://www.mcs.anl.gov/petsc>.
- [39] S. Balay, S. Abhyankar, M. F. Adams, J. Brown, P. Brune, K. Buschelman, L. Dalcin, V. Eijkhout, W. D. Gropp, D. Kaushik, M. G. Knepley, L. C. McInnes, K. Rupp, B. F. Smith, S. Zampini, H. Zhang, H. Zhang, *PETSc Web page*, 2016. URL: <http://www.mcs.anl.gov/petsc>.
- [40] V. E. Henson, U. M. Yang, BoomerAMG: A parallel algebraic multigrid solver and preconditioner, *Appl. Numer. Math.* 41 (2002) 155–177. URL: [http://dx.doi.org/10.1016/S0168-9274\(01\)00115-5](http://dx.doi.org/10.1016/S0168-9274(01)00115-5).
- [41] L. I. G. Kovasznay, Laminar flow behind a two-dimensional grid, *Proc. Cambridge Philos. Soc.* 44 (1948) 58–62. URL: <https://doi.org/10.1017/S0305004100023999>.
- [42] P. Hansbo, M. G. Larson, Piecewise divergence-free discontinuous Galerkin methods for Stokes flow, *Commun. Numer. Meth. Engrg.* 24 (2008) 355–366. URL: <http://dx.doi.org/10.1002/cnm.975>.
- [43] R. Verfürth, A posteriori error estimators for the Stokes equations, *Numer. Math.* 55 (1989) 309–325. URL: <https://doi.org/10.1007/BF01390056>.
- [44] V. Girault, P.-A. Raviart, *Finite Element Methods for Navier–Stokes Equations*, Springer Series in Computational Mathematics, first ed., Springer–Verlag Berlin Heidelberg, 1986.